the $^{11}B$ NMR spectra of the C-substituted (both dimethyl and monomethyl) derivatives of [PPN]**1**.[16]

The observation that $^{2}J(^{205}Tl-^{11}B)$ couplings are much smaller than $^{1}J(^{205}Tl-^{11}B)$ couplings is consistent with the $^{11}B$ NMR spectrum of $[TlMe_2]^+[Me_2TlB_{10}H_{10}]^-$ (**3**).[17] This Tl(III) metallaborane complex exhibits a maximum $^{1}J(^{205}Tl-^{11}B)$ of 258 Hz, which is attributed to the boron nuclei directly bound to the thallium. The large $^{1}J(^{205}Tl-^{11}B)$ values seen in the spectrum of **1** are, to the best of our knowledge, the largest $^{205}Tl$ coupling constants yet observed for a Tl(I) complex.[18] Due to the highly ionic nature of these complexes, there have been only a few spin-spin coupling constants reported.[13] This strong coupling interaction is most likely a direct consequence of the $sp^n$-hybridized bonding orbitals of the dicarbollide ligand. The directional nature and substantial s character possessed by these orbitals would be expected to lead to larger coupling relative to complexes with pure p character in their bonding orbitals (i.e. ligands such as $C_5H_5^-$ and $C_5Me_5^-$).

Calculations concerning the bonding interactions in these thallium dicarbollide complexes have been carried out, and these results together with additional structural and spectroscopic details will be forthcoming in a full paper.

**Acknowledgment.** This work was supported in part by the Office of Naval Research (UCLA) and the Korea Science and Engineering Foundation (KAIST). We would also like to thank Dr. A. Varadarajan for helpful discussions and Andrea Oyeung for the illustrations.

**Supplementary Material Available:** Contour plot of a COSY-90 experiment, details of the synthesis of [PPN]**1**, and tables of crystallographic data collection, atom coordinates and anisotropic thermal parameters, bond distances and angles, and hydrogen atom positions and thermal parameters (8 pages); a table of observed and calculated structure factors (20 pages). Ordering information is given on any current masthead page.

(15) A two-dimensional COSY $^{11}B-^{11}B$ proton-decoupled NMR spectrum of **1** (see supplementary material) supports these assignments through the connectivity pattern established in the contour plot. A single boron gives rise to the doublet with 900-Hz coupling. This boron is directly linked to the 480-Hz doublet. The low-frequency component of the 900-Hz doublet shows off-diagonal correlation with the low-frequency component of the 480-Hz doublet. The same situation exists between the high-frequency components of the two doublets. There are no interdoublet off-diagonal correlations between the low-frequency and the high-frequency components. This same relationship was observed in the 2-D $^{11}B$ NMR spectrum of $[Me_2TlB_{10}H_{12}]^-$ (**3**$^-$).[17] These authors suggested that the absence of any high-frequency/low-frequency component correlation indicates that the relative signs of the observed $^{n}J(^{205}Tl-^{11}B)$ are all the same, presumably positive.

(16) Manning, M. J. Unpublished results.

(17) Beckett, M. A.; Kennedy, J. D.; Howarth, O. W. *J. Chem. Soc., Chem. Commun.* **1985**, 855.

(18) The spin-spin coupling exists irrespective of the choice of solvents (both coordinating and noncoordinating solvents). The choice of cation is not important, and the sparingly soluble parent dithallium complex $Tl^+[TlC_2B_9H_{11}]^-$ also exhibits the coupling in THF. No evidence for coupling to $^{205}Tl$ was seen in the $^1H$ NMR spectrum. Attempts to obtain a $^{205}Tl$ NMR spectrum were unsuccessful, most likely due to coupling of Tl with the quadrupolar boron nucleus.

Department of Chemistry and Biochemistry
University of California, Los Angeles
Los Angeles, California 90024

**Mark J. Manning**
**Carolyn B. Knobler**
**M. Frederick Hawthorne***

Department of Chemistry
Korea Advanced Institute of Science and Technology
Chenongyang, P.O. 150
Seoul, Korea 130-650

**Youngkyu Do**

*Received April 3, 1991*

## Reversible Coordination of Diphenylacetylene to the Dicarbidodecaruthenium Framework. Substitution-Induced Metal-Metal Bond Formation

Much of what is known about high-nuclearity transition-metal carbonyl clusters naturally concerns their preparation and structural characterization;[1,2] only in cases involving especially robust metal frameworks, recent examples being "$Ru_6C$"[3] and "$Re_7IrC$",[4] has systematic derivative chemistry with organic reagents been explored. Prompted in part by a recent report of the degradation of $[Ru_{10}C(CO)_{24}]^{2-}$[5] under mild exposure to carbon monoxide,[6] we wish to present contrasting results with $[Ru_{10}C_2(CO)_{24}]^{2-}$[7] that demonstrate structural integrity for the "$Ru_{10}C_2$" framework under (reversible) substitution by diphenylacetylene.

The reactions of alkynes with high-nuclearity clusters have generally displayed the same features as for smaller clusters, namely, coordination of alkynes as intact molecules to multiple metal centers as well as products resulting from the activation of C≡C or C—H bonds.[1,2,8] Two major types of alkyne ligand-cluster interaction have thus far been recognized, i.e., the insertion of alkynes into metal-metal bonds, resulting in extensive metal framework rearrangement, or $\mu_3$-$\eta^2$-coordination of an alkyne to a triangular face of the original metal polyhedron. The reaction of diphenylacetylene with $[Ru_{10}C_2(CO)_{24}]^{2-}$ (see Scheme I) illustrates a third possible consequence of an alkyne-cluster interaction, namely, coordination-induced metal-metal bond formation. Furthermore, this chemical and structural change is reversed by added carbon monoxide.

$[Et_4N]_2[Ru_{10}C_2(CO)_{24}]$ and diphenylacetylene (ca. 6 equiv) were heated in dry diglyme at 125 °C for 5 days until the growth of a new set of IR ($\nu_{CO}$) bands was complete. After removal of the solvent, the dark purple residue was placed on a deactivated (5% $H_2O$) neutral alumina column. Elution with dichloromethane provided a major purple band, which was collected and crystallized from dichloromethane-diethyl ether at −25 °C to give thin needles (70% yield). Formulation of the product as $[Et_4N]_2[Ru_{10}C_2(CO)_{22}(C_2Ph_2)]$ was based on analytical and spectroscopic data.[9] In the reverse reaction, $[Ph_3PCH_2CH_2PPh_3][Ru_{10}C_2(CO)_{22}(C_2Ph_2)]$[10a] in diglyme was heated at 125 °C under a carbon

(1) Vargas, M. D.; Nicholls, J. N. *Adv. Inorg. Chem. Radiochem.* **1986**, *30*, 123.

(2) Shriver, D. F., Kaesz, H. D., Adams, R. D., Eds. *The Chemistry of Metal Cluster Complexes*; VCH: New York, 1990; especially Chapters 2-5.

(3) (a) Drake, S. R.; Johnson, B. F. G.; Lewis, J.; Conole, G.; McPartlin, M. *J. Chem. Soc., Dalton Trans.* **1990**, 995. (b) Drake, S. R.; Johnson, B. F. G.; Lewis, J. *J. Chem. Soc., Dalton Trans.* **1989**, 243. (c) Chihara, T.; Aoki, K.; Yamazaki, H. *J. Organomet. Chem.* **1990**, *383*, 367. (d) For mention of earlier work see: Bradley, J. S. *Adv. Organomet. Chem.* **1983**, *22*, 1.

(4) (a) Ma, L.; Szajek, L. P.; Shapley, J. R. *Organometallics* **1991**, *10*, 1662. (b) Ma, L.; Wilson, S. R.; Shapley, J. R. *Inorg. Chem.* **1990**, *29*, 5133.

(5) (a) Chihara, T.; Komoto, R.; Kobayashi, K.; Yamazaki, H.; Matsuura, Y. *Inorg. Chem.* **1989**, *28*, 964. (b) Bailey, P. J.; Johnson, B. F. G.; Lewis, J.; McPartlin, M.; Powell, H. R. *J. Organomet. Chem.* **1989**, *377*, C17.

(6) Coston, T.; Lewis, J.; Wilkinson, D.; Johnson, B. F. G. *J. Organomet. Chem.* **1991**, *407*, C13.

(7) (a) Hayward, C.-M. T.; Shapley, J. R.; Churchill, M. R.; Bueno, C.; Rheingold, A. L. *J. Am. Chem. Soc.* **1982**, *104*, 7347. (b) Churchill, M. R.; Bueno, C.; Rheingold, A. L. *J. Organomet. Chem.* **1990**, *395*, 85.

(8) Raithby, P. R.; Rosales, M. J. *Adv. Inorg. Chem. Radiochem.* **1985**, *29*, 169.

(9) Anal. Calcd for $C_{54}H_{50}N_2O_{22}Ru_{10}$ ($[Et_4N]_2$**2**): C, 31.03; H, 2.41; N, 1.34. Found: C, 31.32; H, 2.44; N, 1.30. IR (dichloromethane): $\nu_{CO}$ 2042 (w), 2006 (s), 1999 (vs), 1980 (w, sh), 1927 (w, br), 1812 (w), 1786 (w) cm$^{-1}$. $^1H$ NMR (acetone-$d_6$, 20 °C): $\delta$ 7.26 (m, 10 H, $C_6H_5$), 3.47 (q, 16 H, $J_{H-H}$ = 7.3 Hz, $CH_3CH_2$-), 1.37 (tt, 24 H, $J_{H-H}$ = 7.3 Hz, $J_{N-H}$ = 1.9 Hz, $CH_3CH_2$-). FAB-MS (negative ion, $^{102}Ru$): *m/z* 1968 (M − $Et_4N$).

0020-1669/91/1330-3591$02.50/0 

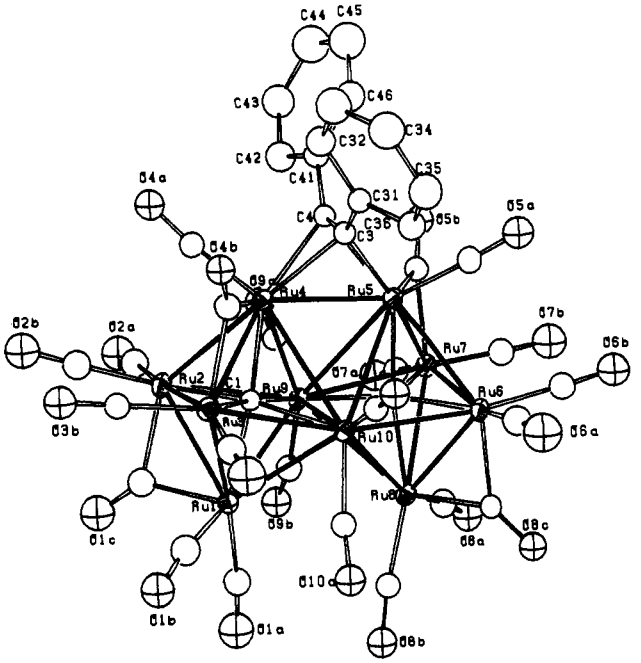


**Figure 1.** Molecular structure of $[Ru_{10}C_2(CO)_{22}(C_2Ph_2)]^{2-}$, showing the atomic labeling scheme.

**Scheme I**

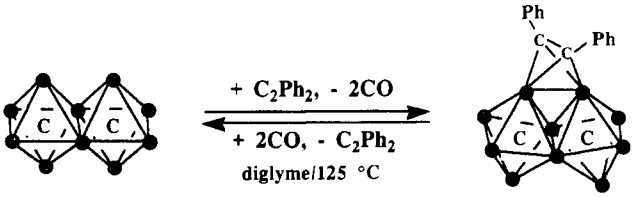


1 2

monoxide atmosphere (20 psig) for 3 days, by which time the solution IR spectrum showed the presence of $[Ru_{10}C_2(CO)_{24}]^{2-}$ alone.

An X-ray crystallographic study of $[Ph_3PCH_2CH_2PPh_3]^{2+}$ salt[10] revealed the solid-state structure of the anion as shown in Figure 1. The overall geometry adopted by the 10 ruthenium atoms is based on the edge-sharing bioctahedral framework as in the parent **1**,[7] with the two carbide ligands occupying the octahedral interstitial positions. The diphenylacetylene ligand is bonded to two neighboring apical ruthenium atoms, Ru4 and Ru5, with the carbon–carbon vector perpendicular to the Ru4–Ru5 vector. The carbon–carbon bond distance is 1.30 (2) Å. The two phenyl groups are bent away from the ruthenium framework, forming equal C31–C3–C4 and C41–C4–C3 angles of 139 (1)°. As in the parent ion **1**, there are four edge-bridging carbonyl ligands positioned in a pairwise fashion on four of the eight edges involving apical to "nonhinge" equatorial ruthenium atoms. Each ruthenium atom is also bound to two terminal carbonyl ligands, except for the two acetylene-bridged apical ruthenium atoms Ru4 and Ru5, which have but one terminal carbonyl each.

Although diphenylacetylene substitution into **1** causes minimal perturbation of the carbonyl ligand sphere and does not change the gross features of the bioctahedral metal framework, some of the metal–metal distance changes are noteworthy. The most striking feature is the shortening of one apical–apical distance (Ru4–Ru5 = 2.711 (1) Å), and the elongation of the other (Ru1–Ru8 = 3.823 (1) Å, compared with 3.122 (2) and 3.138 (2) Å in **1**) as the result of the diphenylacetylene coordination. The six equatorial ruthenium atoms do not share the same plane, and a folded structure, with a hinge angle of 161°, is observed. The average Ru–C (carbide) distance, however, is essentially unchanged (2.06 Å in **2** vs 2.07 Å in **1**). Since the total electron counts of **1** and **2** are the same (both have 138 valence electrons), according to the cluster electron counting rules,[2,11] the formation of the Ru4–Ru5 bond should be compensated by the loss of a bonding interaction within the octahedra. Examination of the Ru–Ru distances of **2** reveals both bond shortenings and bond lengthenings compared to **1**.[12] The four nonbridged apical–equatorial bonds show an average decrease of 0.076 Å, and the Ru9–Ru10 hinge distance is shortened from 2.872 (1) Å to 2.765 (1) Å. The most noticeable elongations occur at the two equatorial–equatorial bonds. The specific set of apical–hinge distances involving Ru4 and Ru5 are longer than the rest of the intraoctahedral bonds, with the Ru5–Ru9 bond being the longest (3.125 (1) Å) in the cluster. However, the average of all apical–hinge distances for **2** is only slightly larger than the corresponding value for **1**. Thus, on the basis of metal–metal bond distances, there is no sign of a localized pair of antibonding electrons.

It has been pointed out previously that certain structural features of **1** can be rationalized by considering its total valence electron count.[7] Specifically, the count of 138 electrons is four greater than that calculated for an edge-fused bioctahedral structure with full bonding interactions between the two pairs of apical positions. In the actual structure, these two extra pairs of electrons appear to be largely localized on the apical positions, reducing the net apical–apical bonding formally to zero, and leading to nonbonded apical–apical repulsions. Symmetrical loss of two carbonyl ligands, thereby reducing the electron count to 134, could restore the apical–apical bonding interactions (see I). However, an alternative possibility is the less symmetrical loss of two carbonyl ligands from just the "top" of the structure. Concomitant folding of the framework at the fused positions could allow the formation of a multiple bond between the top two apical positions and lead to the elimination of nonbonded repulsions between the bottom two apical positions (see II). From this point of view the formation of the acetylene adduct **2** would be similar to formation of dimetallatetrahedrane complexes from the interaction of dinuclear metal–metal multiple bonded systems with alkynes, in particular,

I II

(10) (a) An acetone solution (5 mL) of $[Et_4N]_2$**2** (ca. 10 mg) was mixed with a methanol solution (5 mL) of $[Ph_3PCH_2CH_2PPh_3]Br_2$ (120 mg), resulting in the formation of purple microcrystals. Crystallization from acetone–methanol at −25 °C gave diffraction quality crystals. (b) Crystallographic data for $[Ph_3PCH_2CH_2PPh_3]$**2**·$CH_3OH$·$2(CH_3)_2CO$: monoclinic, space group $P2_1/n$, $a$ = 16.552 (4) Å, $b$ = 26.923 (8) Å, $c$ = 19.424 (4) Å, $\beta$ = 90.89 (2)°, $V$ = 8655 (6) Å$^3$, $Z$ = 4. (c) Data collection was carried out at −50 °C on an Enraf-Nonius CAD4 automated $\kappa$-axis diffractometer. A total of 7837 reflections with $I > 2.58\sigma(I)$ were corrected for absorption ($\mu$(Mo K$\alpha$) = 17.70 cm$^{-1}$; max/min transmission factors = 0.643/0.421) and used for solving the structure by direct methods (SHELX-86). Positions for the ruthenium atoms were deduced from an $E$ map. Subsequent least-squares refinement and difference Fourier syntheses (SHELX-76) revealed positions for the remaining non-hydrogen atoms, including one methanol and two acetone solvate molecules. Host molecule hydrogen atoms were included as fixed contributors in idealized positions, and phenyl rings were refined as ideal rigid groups. One acetone solvate was disordered and was constrained to ideal geometry, and the relative site occupancies for molecules "A" and "B" converged to 0.395 (7) and 0.605 (7). In the final cycle of least-squares refinement, common isotropic thermal parameters were varied for disordered acetone and hydrogen atoms, anisotropic thermal coefficients were refined for the ruthenium atoms, and independent isotropic thermal coefficients were refined for the other non-hydrogen atoms. Final agreement factors were $R$ = 0.049 and $R_w$ = 0.057.

(11) Mingos, D. M. P. *Acc. Chem. Res.* **1984**, *17*, 311.

(12) For the convenience of comparison, the average Ru–Ru distances (Å) are listed here (the values for $[Ru_{10}C_2(CO)_{24}]^{2-}$ are given in parentheses): (1) CO bridged apical–equatorial, 2.783 (2.813); (2) nonbridged apical–equatorial, 2.907 (2.983); (3) apical–hinge, 2.995 (2.976); (4) hinge–hinge, 2.765 (2.872); (5) equatorial–hinge, 2.912 (2.902); (6) equatorial–equatorial, 3.004 (2.940); (7) apical–apical, 3.267 (3.130).

the well-studied $Cp_2Mo_2(CO)_4$ system.[13] Although there is no evidence at this stage for a multiply bonded intermediate in the $Ru_{10}C_2$ chemistry, we are actively pursuing the implications of this analogy.

**Acknowledgment.** This work was supported by National Science Foundation Grant CHE 89-15349 and its predecessors. L.M. is grateful to the Department of Chemistry for fellowship support during 1988-1991. We thank a reviewer of an earlier version of this work for suggesting that the substitution reaction be checked for reversibility.

**Supplementary Material Available:** Tables of the details of crystallographic data collection, atomic coordinates, hydrogen atom parameters, thermal parameters, and selected bond distances and angles for $[Ph_3PCH_2CH_2PPh_3][Ru_{10}C_2(CO)_{22}(C_2Ph_2)]\cdot CH_3OH\cdot 2(CH_3)_2CO$ (15 pages); a table of observed and calculated structure factors (27 pages). Ordering information is given on any current masthead page.

(13) Curtis, M. D. *Polyhedron* **1987**, *6*, 759.

School of Chemical Sciences
University of Illinois
Urbana, Illinois 61801

**Linqing Ma**
**Damian P. S. Rodgers**
**Scott R. Wilson**
**John R. Shapley***

*Received April 11, 1991*

## Labile and Coordinatively Unsaturated Molybdenum(III)-μ-Sulfido Dimers, $Mo_2(\mu\text{-}S)(\mu\text{-}Cl)Cl_3(PMe_3)_4(L)$ (L = $PMe_3$, MeCN, or Vacant), Formed by Sulfur Atom Abstraction from $SPMe_3$

Three novel molybdenum(III) dimers are reported here, two with edge-shared bioctahedral structures and one with an unprecedented coordinatively unsaturated structure. Facile ligand exchange reactions interconvert the three molecules. While complexes with two metal atoms have been widely studied[1-3] (for instance, there are 93 examples of edge-shared bioctahedral dimers, according to a recent paper[4]), molecules with an open coordination site and/or labile ligands are rare. The synthesis of these compounds, by sulfur atom transfer from $SPMe_3$ to Mo, is also remarkable because phosphines typically remove sulfur from metal complexes, due to the strength of the P-S bond (≅92 kcal/mol[5]).

Reaction of toluene solutions of $MoCl_2(PMe_3)_4$ (**1**)[6] with $^1/_2$ equiv of $SPMe_3$ for 1 day at 80 °C results in the formation of $Mo_2(\mu\text{-}S)(\mu\text{-}Cl)Cl_3(PMe_3)_5$ (**2**) along with 4 equiv of free $PMe_3$ (Scheme I). The reaction is slowed by the buildup of free $PMe_3$ and requires removal of the phosphine to proceed to completion. When the isolated dark blue-green solid is repeatedly triturated with solvent and stripped of volatiles in vacuo, 1 equiv of bound $PMe_3$ is lost, resulting in the formation of brown $Mo_2(\mu\text{-}S)(\mu\text{-}Cl)Cl_3(PMe_3)_4$ (**3**) in high yield (>95% by NMR). Because **2** loses $PMe_3$ so easily, pure samples are best prepared by recrystallization of **3** in the presence of $PMe_3$. Thus **2** and **3** + $PMe_3$ readily interconvert, as confirmed by NMR studies (see below) and by visible spectroscopy: addition of $PMe_3$ to brownish amber **3** forms blue-green **2**, which is converted back to **3** by the phosphine scavenger $ZnCl_2$. Dissolution of **3** in acetonitrile yields a navy blue adduct, $Mo_2(\mu\text{-}S)(\mu\text{-}Cl)Cl_3(PMe_3)_4(CH_3CN)$ (**4**; Scheme I). Addition of benzene or toluene to **4** causes loss of the coordinated $CH_3CN$ and forms **3**, indicating a similar **3** ⇄ **4** equilibrium.

All three dimers have been characterized by single-crystal X-ray diffraction (Figures 1-3).[7] Complexes **2** and **4** have the edge-shared bioctahedral structure (Scheme I) that is typical of $M_2L_{10}$ compounds,[2,3a-c] but **3** has a unique structure in which one molybdenum is only five-coordinate and coordinatively unsaturated.

**Scheme I.** Syntheses and Interconversion of $Mo_2(\mu\text{-}S)(\mu\text{-}Cl)Cl_3(PMe_3)_4L'$ Compounds (L' = $PMe_3$ (**2**), Nothing (**3**), MeCN (**4**) [L = $PMe_3$])

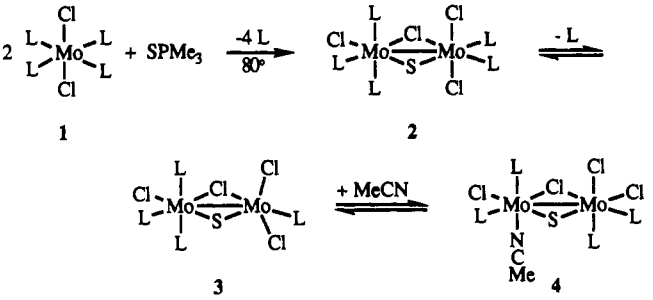


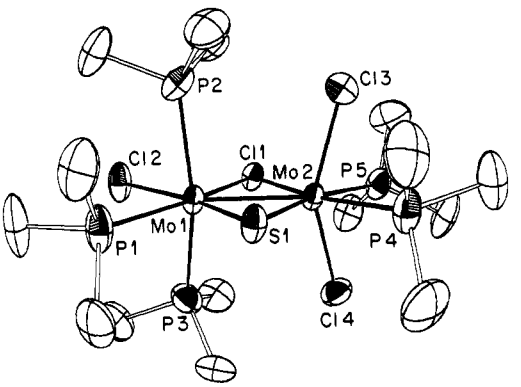


**Figure 1.** ORTEP drawing of $Mo_2(\mu\text{-}S)(\mu\text{-}Cl)Cl_3(PMe_3)_5$ (**2**) with 40% probability thermal ellipsoids. Selected bond distances (Å) and angles (deg) are as follows: Mo(1)-S(1) = 2.2740 (13), Mo(2)-S(1) = 2.2852 (13), Mo(1)-Cl(1) = 2.4360 (12), Mo(2)-Cl(1) = 2.4427 (12); Mo(1)-S(1)-Mo(2) = 72.49 (4), Mo(1)-Cl(1)-Mo(2) = 67.08 (3), P(2)-Mo(1)-P(3) = 164.08 (6), Cl(3)-Mo(2)-Cl(4) = 150.42 (6).

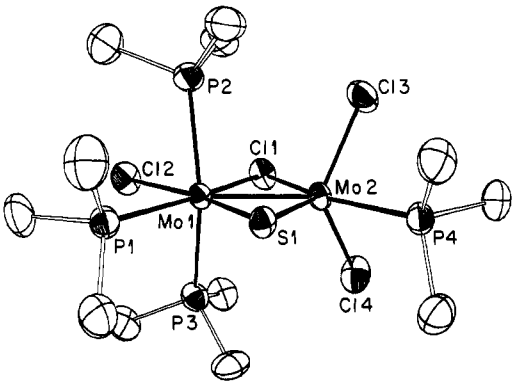


**Figure 2.** ORTEP drawing of $Mo_2(\mu\text{-}S)(\mu\text{-}Cl)Cl_3(PMe_3)_4$ (**3**) with 40% probability thermal ellipsoids. Selected bond distances (Å) and angles (deg) are as follows: Mo(1)-S(1) = 2.288 (2), Mo(2)-S(1) = 2.222 (2), Mo(1)-Cl(1) = 2.492 (2), Mo(2)-Cl(1) = 2.438 (2); P(2)-Mo(1)-P(3) = 165.87 (7), Cl(3)-Mo(2)-Cl(4) = 124.13 (8), Cl(1)-Mo(2)-P(4) = 166.26 (8).

(1) Cotton, F. A.; Walton, R. A. *Multiple Bonds Between Metal Atoms*; Wiley-Interscience: New York, 1982.
(2) Cotton, F. A. *Polyhedron* **1987**, *6*, 667-677.
(3) (a) Messerle, L. *Chem. Rev.* **1988**, *88*, 1229-1254. (b) Shaik, S.; Hoffman, R.; Fisel, C. R.; Summerville, R. H. *J. Am. Chem. Soc.* **1980**, *102*, 4555. (c) Poli, R.; Mui, H. D. *Inorg. Chem.* **1991**, *30*, 65-77. (d) Cotton, F. A.; Ucko, D. A. *Inorg. Chim. Acta* **1972**, *6*, 161-172. (e) Hoffman, R.; Summerville, R. H. *J. Am. Chem. Soc.* **1979**, *101*, 3821-3831.
(4) Cotton, F. A. *Inorg. Chem.* **1990**, *29*, 4002-4005.
(5) Chernick, C. L.; Pedley, J. B.; Skinner, H. A. *J. Chem. Soc.* **1957**, 1851.
(6) Rogers, R. D.; Carmona, E.; Galindo, A.; Atwood, J. L.; Canada, L. G. *J. Organomet. Chem.* **1984**, *277*, 403-415.
(7) Crystal data: for $2\cdot{}^1/_6\,C_7H_8$, $R\bar{3}$ (hexagonal setting), $a$ = 18.840 (6) Å, $c$ = 49.989 (5) Å, $Z$ = 18, $V$ = 15058.8 (11) Å$^3$, $R$ = 3.5%, $R_w$ = 4.7%, GOF = 1.047; for $3\cdot C_7H_8$, $C2/c$, $a$ = 37.822 (5) Å, $b$ = 9.6820 (9) Å, $c$ = 22.249 (3) Å, $\beta$ = 125.48 (1)°, $Z$ = 8, $V$ = 6635 (3) Å$^3$, $R$ = 4.3%, $R_w$ = 4.4%, GOF = 1.324; for **4**, $P\bar{1}$, $a$ = 8.578 (1) Å, $b$ = 10.176 (1) Å, $c$ = 17.562 (2) Å, $\alpha$ = 101.04 (1)°, $\beta$ = 95.54 (1)°, $\gamma$ = 106.89 (1)°, $Z$ = 2, $V$ = 1420.7 (7) Å$^3$, $R$ = 3.6%, $R_w$ = 4.3%, GOF = 1.114.

0020-1669/91/1330-3593$02.50/0 